Statistical Comparison of the Baseline Mechanical Properties of Imerys and RSM Graphite

Paul Adams, University of Sheffield, United Kingdom

December 2021

Prepared for:

Sheriozha Anthony Wijekoon, Director & CEO, RS Mines

.

Introduction

High-purity graphite is a core structural material of choice in EV electrode design.

This baseline graphite characterisation report looks to compare the mechanical and physical properties of graphite from a typical supplier, Imerys, and that from RS Mines. Comprehensive data is enclosed that captures the level of variation in measured values. In addition to providing a comprehensive comparison between values in the different graphites, the report also carefully tracks individual specimen sources, position, and orientation information to provide comparisons in specific properties.

An analysis of the comparison between these two graphites will include not only the differences in fundamental and statistically significant individual strength levels, but also the differences in variability in properties within each of them that will ultimately provide the basis for the prediction of performance. The comparative performance of the different types of graphites will continue to evolve as more specimens are fully characterized from the numerous grades of future graphite being evaluated.

The comparison at this early stage is relatively simple. I will look at Physical Properties and Mechanical Properties – Tensile Testing, Flexural Testing and Compressive Testing. A positive return on these fundamental properties in a side by side comparison, creates a strong correlation between these patterns and strong suitability for EV electrode material components.

PHYSICAL PROPERTIES

A qualitative comparison between the graphites was observed through a 3D representation of the original samples that reflects property data based upon the measured value (colour) and actual position within the sample. Image A below shows the density values measured in both Imerys and RSM, from which it is clear that the density of the RSM graphite has an end-to-end variability based upon the relative range of values measured as well as a slight inside-outside gradient with higher density values nearer the sample surface. A more quantitative representation of the range of values is made through a probability distribution, as is shown in IMAGE 2, which utilises an appropriate curve fit to determine a characteristic value based upon the distribution as well as a quantitative measurement of the shape parameter, or degree of variability in the overall population, based on the slope of the distribution. In the case of density measurements on flexural and compressive mechanical test specimens, the RSM graphite exhibits less overall variability in the distribution (and therefore greater predictability) based upon the higher slope value than is shown by the Imerys distribution. The RSM sample clearly demonstrates a higher density.

IMAGE A

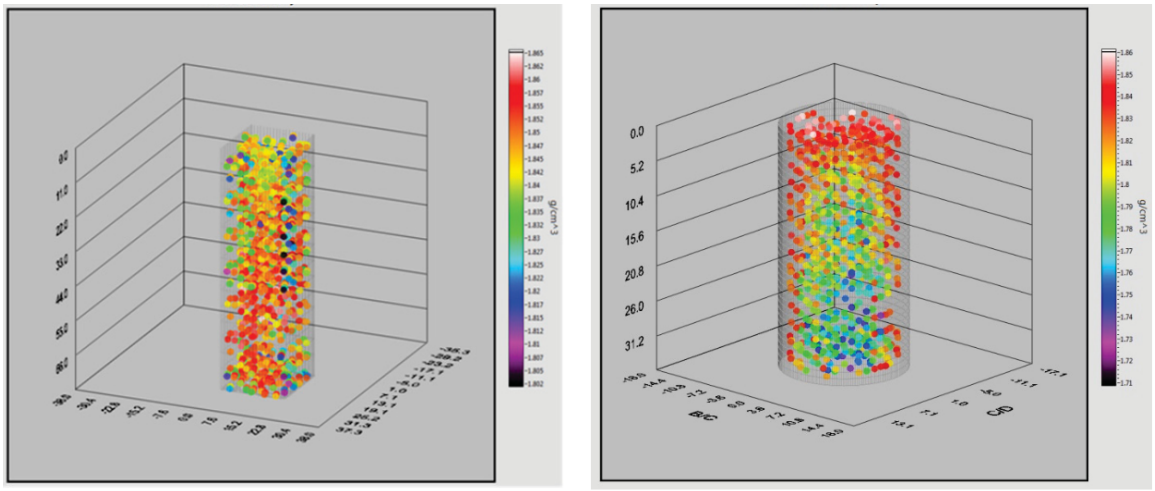

RSM **Imerys**

IMAGE B

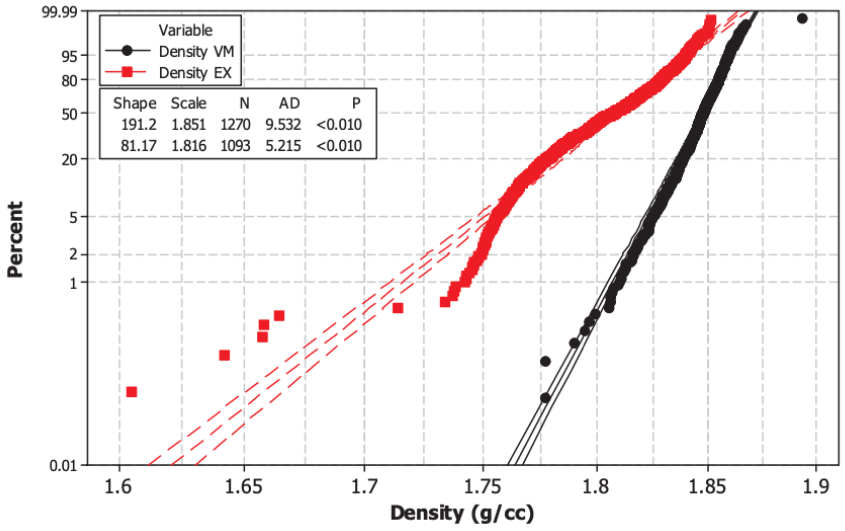

Image C is a comparison between the elastic and shear moduli in Imerys and RSM measured via resonant frequency measurements in flexural bars. Image D shows the variation between values in individual samples of each grade. As can be seen from the figures, the variability in Imerys graphite is higher than that seen in the RSM grade.

IMAGE C

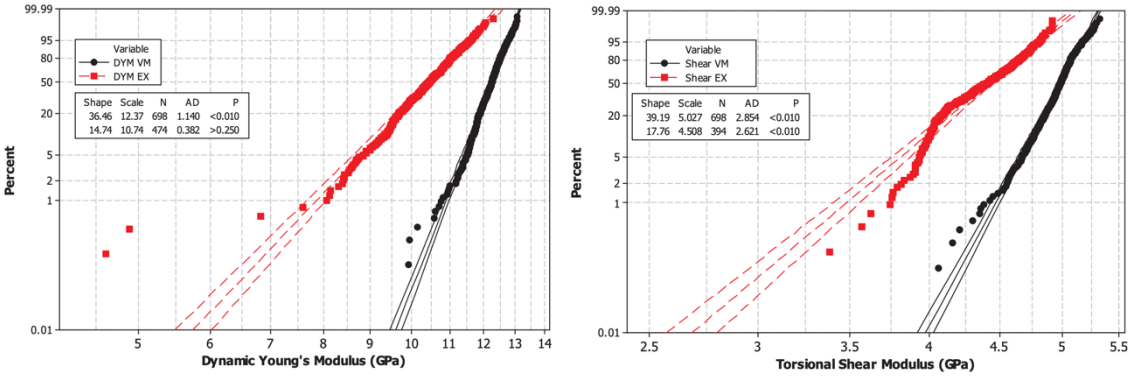

Image C shows a Dynamic YM and Torsional Shear moduli comparison of Imerys and RSM graphite samples. RSM is represented by the black line, Imerys by the red line.

IMAGE D

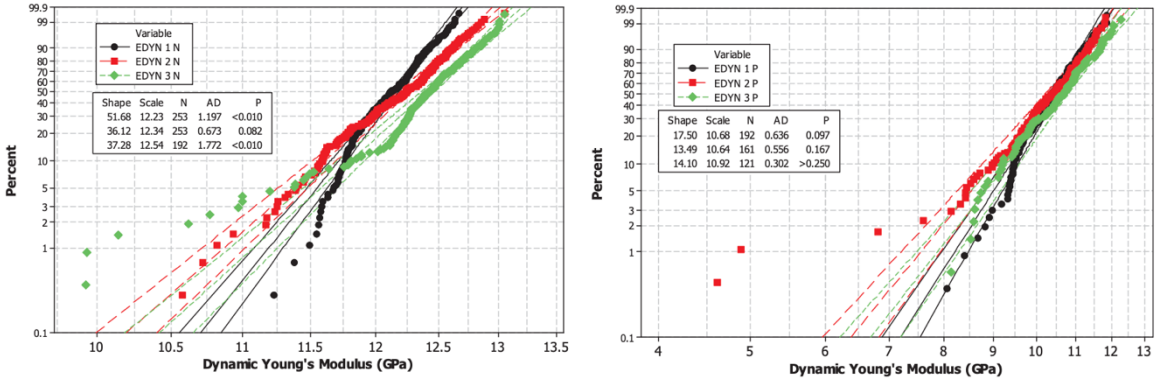

Dynamic Young's modulus comparison between the individual samples of RSM graphite (left) and Imerys graphite (right). The RSM graphite (plotted on a much tighter x-axis scale) exhibits considerably less modulus variability. This is surprising considering the raw nature of the RSM samples.

The same elastic constants can be evaluated through other means. In this work, sonic velocity measurements are used to evaluate those elastic constants using compression specimens (Image E). The data shows a similar trend in the difference between the graphites, with the RSM graphite exhibiting higher stiffness and an overall lower variability in the distribution of values.

IMAGE E

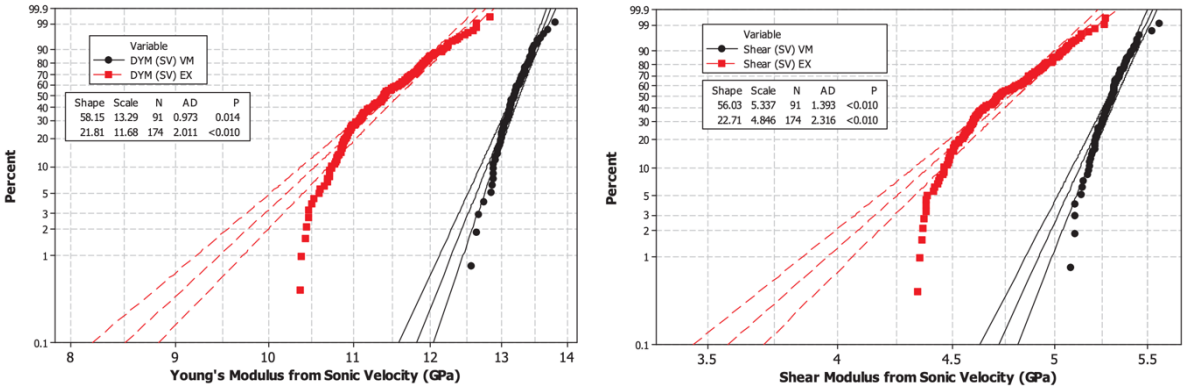

Young's modulus (left) and shear modulus (right) comparisons between the grades reveal similar higher stiffness values and a tighter distribution for the RSM grade, with the individual data points (both modulus types were taken from each specimen measured) indicating similar values from each specimen based upon the similar distribution shapes.

Another key characteristic in evaluating the inherent flaw distribution in the material is the comparison of these elastic constants, presumably similar, that were obtained using different techniques. As shown in Image F, a direct comparison of the calculated Young's modulus based on sonic velocity and resonant frequency measurements for each graphite exhibits a different degree of variability. The distributions for both graphites exhibit considerably less variability for the modulus of the material based upon sonic velocity measurements, despite the fact that both techniques are measuring the same material parameter.

The result is indicative of the effect of flaw and void population on the transmission of vibrations that are resonating in the specimen volume vs. the interaction of those same flaws and the associated attenuation of a planar sound wave. The individual techniques can provide additional information as to the character of the flaw and void distribution in graphite through a comparison of the same physical property.

IMAGE F

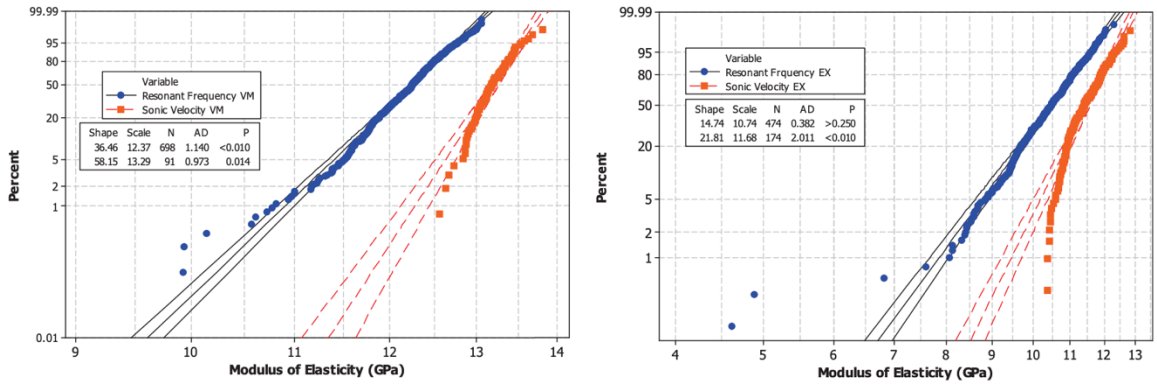

A comparison of the modulus of elasticity (Young's modulus) for RSM (left) and Imerys (right) grades of graphite using two different measurement techniques. The modulus by sonic velocity exhibits considerably less variability and a lower incidence of low-value outliers.

MECHANICAL PROPERTIES

Tensile Testing

The qualitative tensile property comparison between samples of RSM and Imerys is shown in Image G. A similar trend in variability from end to end can be seen in the Imerys graphite that was seen in the density values. An overall comparison of tensile strength values via a probability distribution is shown in Image H, along with the relative differences between samples of the same grade. When considering the qualitative variability seen, further partitioning of the data into logical subsets will allow a more thorough determination of the degree of variability along this sample axis. Image I is a boxplot of the distribution of tensile strength values based upon groupings by layer along the long axis, which is one of the position axes that reveals a demonstrable within-sample gradient.

IMAGE G

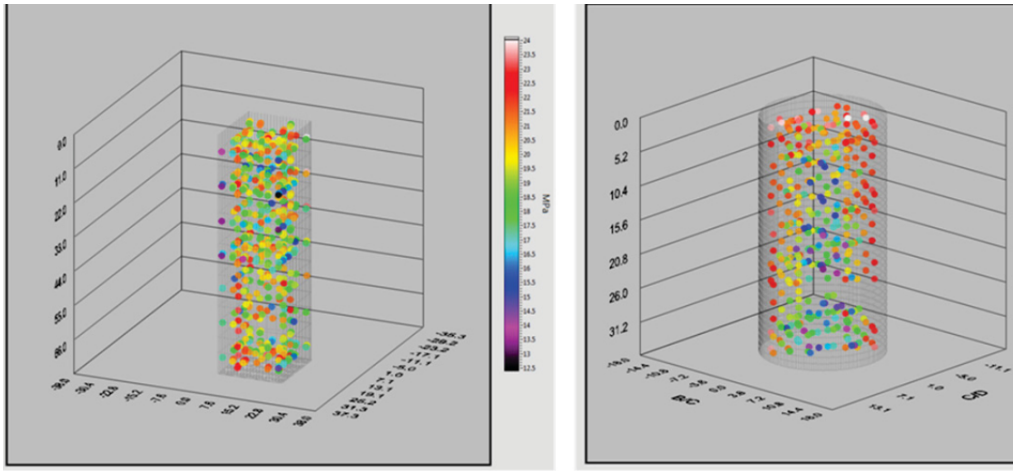

RSM **Imerys**

A qualitative 3D representation of the distribution of tensile strength values in RSM (left) and Imerys (right) graphite grades. The gradient in the Imerys graphite is reflective of the same pattern in the density distributions analysis

IMAGE H

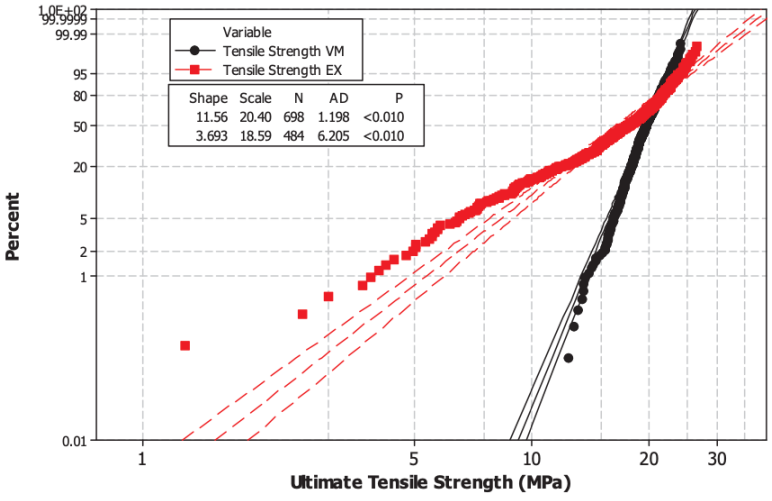

Weibull distributions of the tensile strengths measured in each grade show a higher characteristic value of 20.40 MPa for the RSM grade vs. 18.59 MPa for the Imerys grade, despite the upper values for the Imerys grade being higher. The overall distribution shows less variability at a higher overall mean value for the RSM grade.

IMAGE I

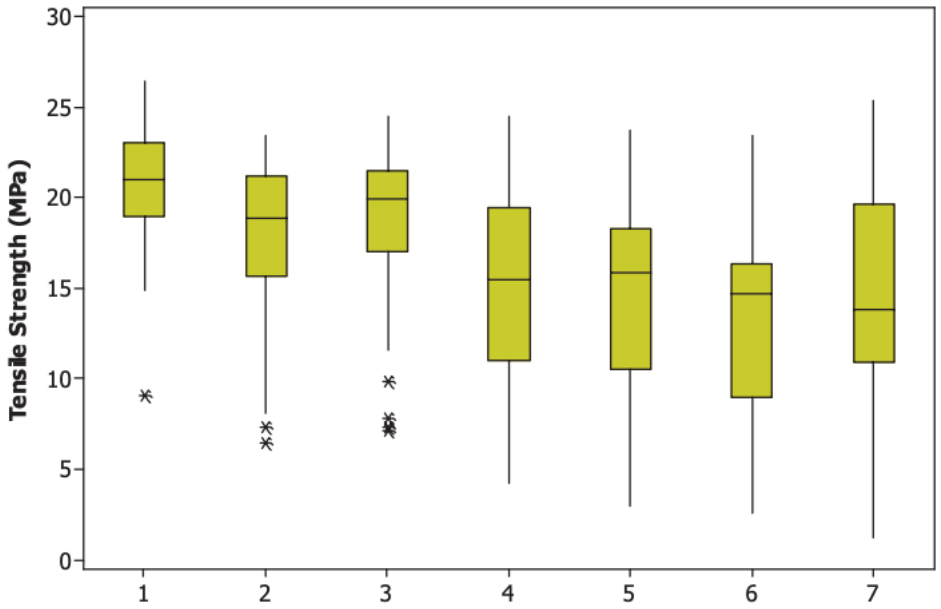

The same relative drop in tensile strength values from end to end can be seen based upon 7 distinct sample- based groupings obtained from the same positions in all three of the samples being evaluated. To ensure that the behaviour is consistent across samples, the same evaluation can be made through further breaking down the subsets of data by individual sample. While the general trend is confirmed, it was observed that the extensive breakdown of data into smaller subsets begins to compromise the statistical significance of the resulting dataset. The trend in strength from end to end in the individual Imerys samples is not as clearly discernible, as the variability in each dataset increases along with the relative overlap between mean values in each of the samples. In a complementary manner, the relative strength trend in the RSM graphite that is not seen in similarly sized data populations may be too subtle to be identified using the data collected to date, but, if it exists, may manifest itself as more data is collected on that grade and integrated into the full-grade representations. With the present tensile data collected on RSM samples, no statistically significant variation is seen.

The effect of orientation on mechanical properties is also important, as shown in Image J. The major orientations of interest from a global perspective in graphite are based upon the atomic level configuration of the graphite unit cell. The “with-grain” direction is along the *a* direction, or plane of hexagonal carbon atoms, while the *c* direction is perpendicular to the planes, in the direction of the stacked layers. In Imerys graphite, the with-grain direction is assumed to be predominant along the extrusion axis. RSM sampling results in a settling of the planar orientations that is predominant along the short axis of the sample, which is orthogonal to the long axes as they rest on the vibrating plane during molding. For practical purposes, these orientations are captured in the datasets although the respective processes result in nearly isotropic distributions. From a more application-specific evaluation, the comparisons are made based upon the major orientations within the original samples identified later in this report.

IMAGE J

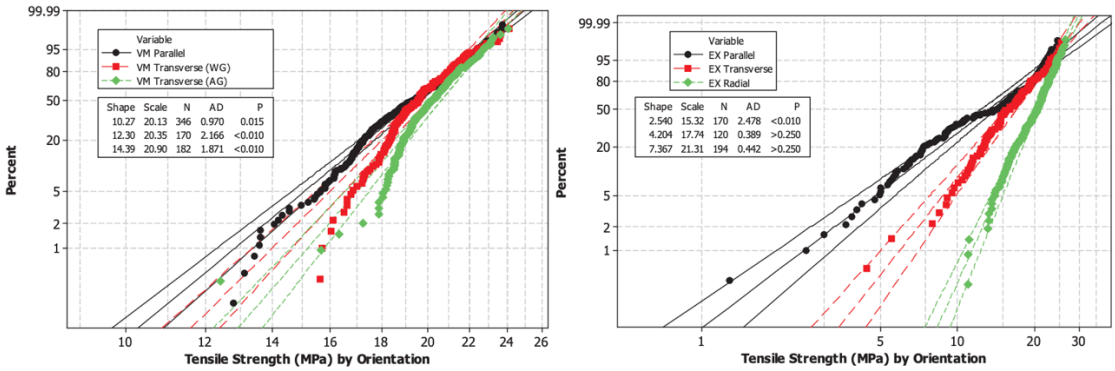

The variability between orientations is more pronounced in the Imerys grade, with the radial orientation exhibiting the highest strength. The distribution of values is much closer in the RSM grade, with the highest characteristic value for strength being shown by the orientation commonly regarded as the weakest – the against-grain orientation.

The Young's modulus of the material can also be evaluated through the direct stress-strain relationship captured during the execution of individual tensile tests, utilizing the two axes being plotted and applying the YM relationship. A comparison can be made between the test techniques used to capture the same material property – this time including the mechanical stress-strain response as a direct comparator to the physical property data captured through impulse excitation (vibration) or sound wave propagation. As is shown in the top of Image K the stress/strain data yields the lowest stiffness values and highest overall variability, likely owing to the larger population of specimen flaws being captured in the gauge volume under test.

IMAGE K

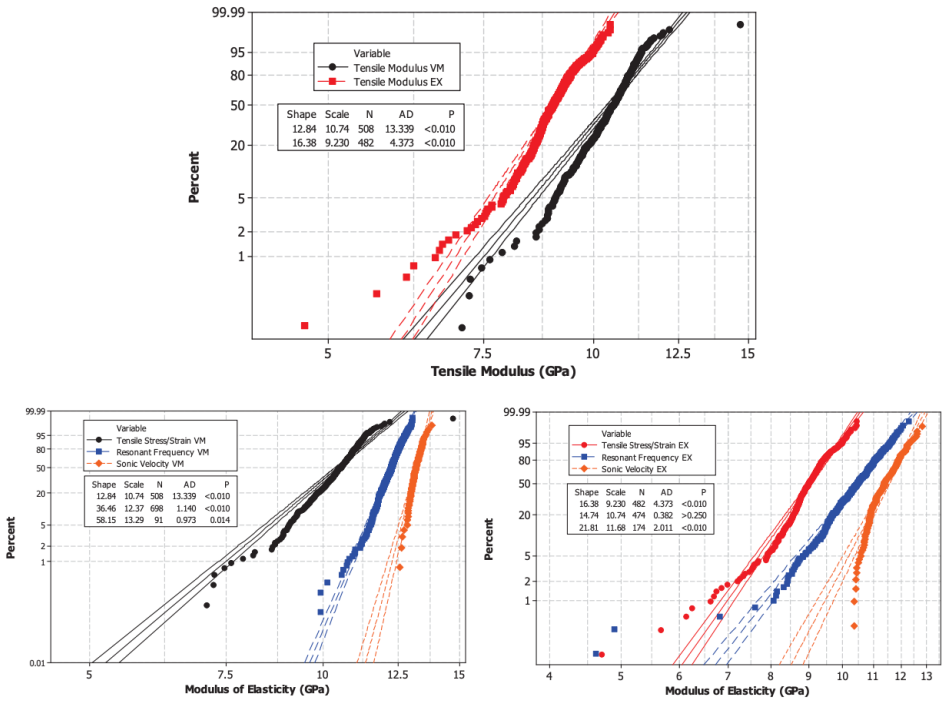

As with the physical property measurements, the RSM grade exhibits higher stiffness across the distribution of values (top). The comparison of test techniques to resulting values further illustrates the effects of test method on the parameter being evaluated; the modulus by stress/strain measurements is consistently lower than the non-destructive techniques (resonant frequency and sonic velocity) presented in the previous section.

Flexural Testing

The qualitative comparison of flexural strength based upon the specific grades being evaluated and the relative position within the sample is shown in Image L. As with the density and tensile strength results, the Imerys grade shows a distinct property gradient through the volume of the overall sample. The associated probability distribution based upon the total amount of flexural strength data points for each grade is shown in Image M. The low-strength outliers are more prevalent in the Imerys grade than in the RSM grade, and the variability in the dataset is much wider. There is a distinct crossover in flexural strength between the two grades, with a maximum flexural strength in the Imerys grade at nearly 38 MPa while the maximum flexural strength in RSM grade is just under 33 MPa.

IMAGE L

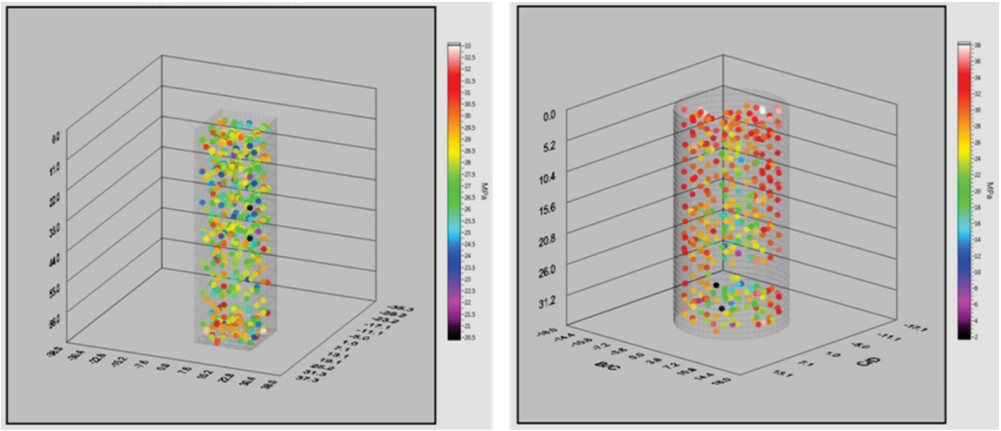

3D representation of flexural strength results for each of the two grades shows a more homogeneous distribution for the RSM graphite than for the Imerys grade, which further reflects the gradients seen in the density distribution earlier in this report.

IMAGE M

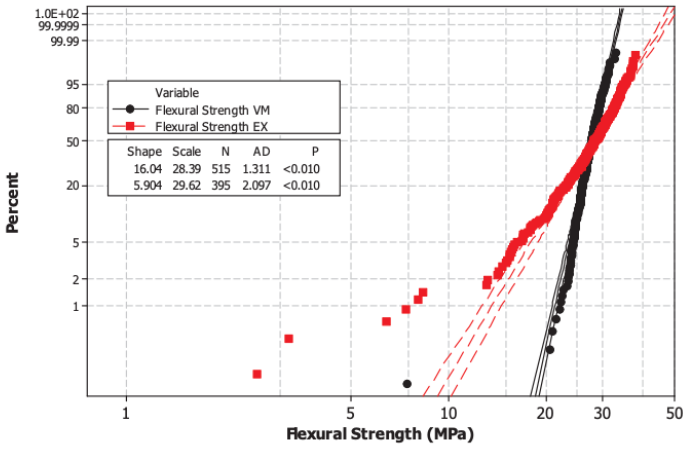

The flexural strength values are similar in distribution to the tensile test results, exhibiting a crossover region at the higher values for the Imerys graphite. Unlike the tensile results, the characteristic value for flexure strength is higher for the Imerys grade despite the larger range of variability in that grade, particularly at the low strength values. This is to be expected for a refined product that is “in market” relative to the raw RSM material.

IMAGE N

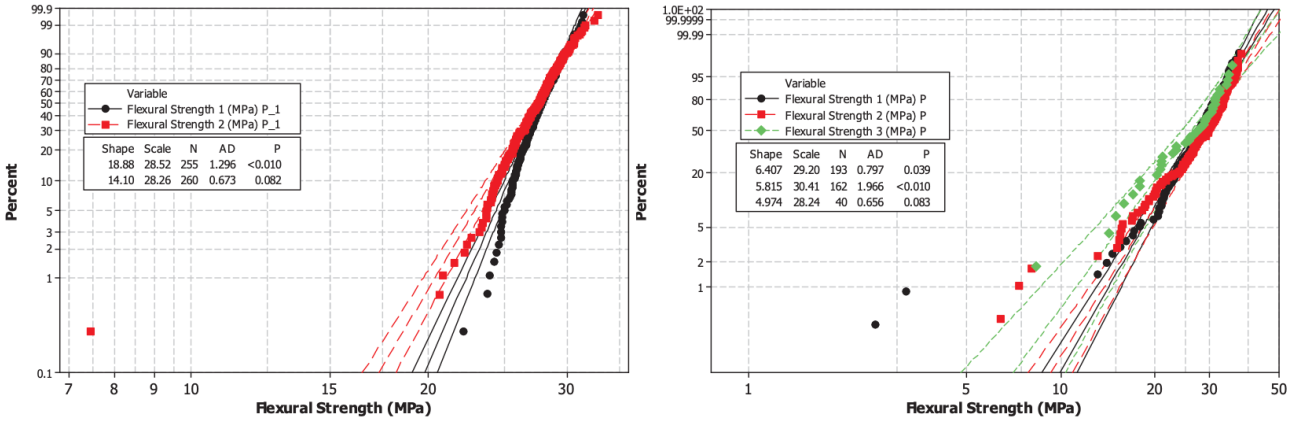

Flexural strength between samples of the same grade for two RSM (left) and three Imerys (right) graphite samples.

The within-grade variability is shown in Image N. As can be seen from the image, the variability (slope) of the distribution is consistent between grades, and reflective of the overall distribution seen in the total distribution plot shown in Image M. Outside of the single low outlier value exhibited in the second RSM sample, the probability distributions are relatively consistent within the RSM grade when compared to the Imerys grade.

The shift in flexural strength values from sample end to sample end is also seen in the Imerys graphite to an extent not seen in the RSM grade. Image O shows comparison boxplots of flexural strength as grouped by *z*-axis sample number that reflect the decrease in values from one end to the other. Although the shift is not as distinct from end to end as seen in density and tensile strength grouped values, it is clearly prevalent when compared to the same boxplot for the RSM grade, which shows no significant variability in mean values. An analysis of variance (ANOVA) evaluation (Image O) shows an even more clear decreasing trend in values through the length of the sample. The associated P-value for mean values of flexural strength by sample in the Imerys sample is well below 0.05 (95% confidence interval), indicating that a difference in the mean values based upon this decreasing trend is statistically significant.

A comparison of orientation effects between the two grades is shown in Image P. The relative variability between orientations in the RSM grade is fairly consistent; both the characteristic values and distribution slope of each is similar. More disparity exists in the Imerys grade, with the radial orientation having the most consistent and highest mean flexural strength values. As with the parallel orientation in tensile testing, the parallel orientation exhibits the highest amount of variation and the lowest mean strength in flexure.

IMAGE O

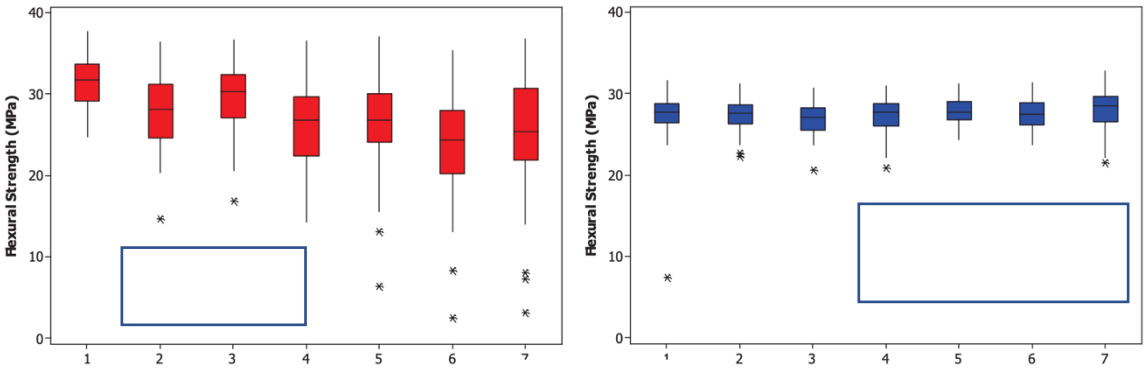

IMERYS **RSM**

The end-to-end variability and general spread in data is clear in the Imerys grade, with values decreasing by z- axis length via sample number groupings. The RSM grade exhibits a similar mean value throughout.

IMAGE P

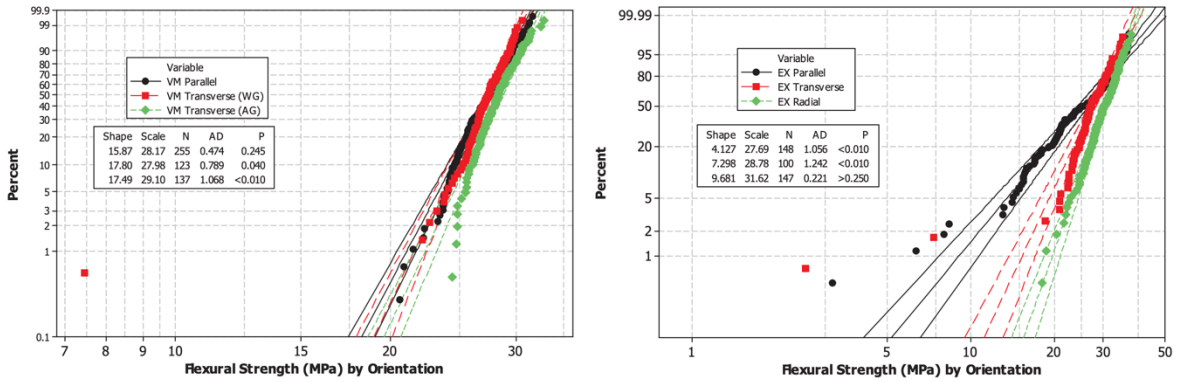

Flexural strength by orientation in each of the grades exhibits similar results to the tensile data. In the RSM graphite, the results in each of the orientations is similar, with the against-grain orientation showing the highest strength value for the distribution. The radial orientation is the strongest in the Imerys grades, while the parallel orientation is weakest.

Compressive Testing

A similar qualitative comparison of compressive strength to that shown for both tensile and flexural strengths, demonstrating the comprehensive value distributions based upon the specific grades being evaluated and the relative positions within the sample, is shown in Image Q. As with the other mechanical test values, the pattern that emerges is a relatively homogeneous distribution of values in the RSM grade, with an end-to-end and inside-outside decreasing strength trend in the Imerys grade, particularly along the centreline of the sample. The overall distribution of compressive strength values is shown in Image R. A number of key features are captured in this image; first, as in other graphites, the compressive strength is significantly higher than that in tension or bending, with mean values for stress levels increasing by a factor of roughly 2 to 4 of the tension-based failure of tensile and flexural testing. Second, similar to the tensile and flexure test results, the data scatter is significantly higher in compression for the Imerys grade, with a variability shape factor that decreases from just under 20 for the RSM grade to 7 for the Imerys grade. Unlike the tensile and flexure results, no crossover in maximum values exists between the two grades – the RSM graphite is higher in compressive strength throughout the data distribution. Both the maximum and minimum values are higher for the RSM grade.

IMAGE Q

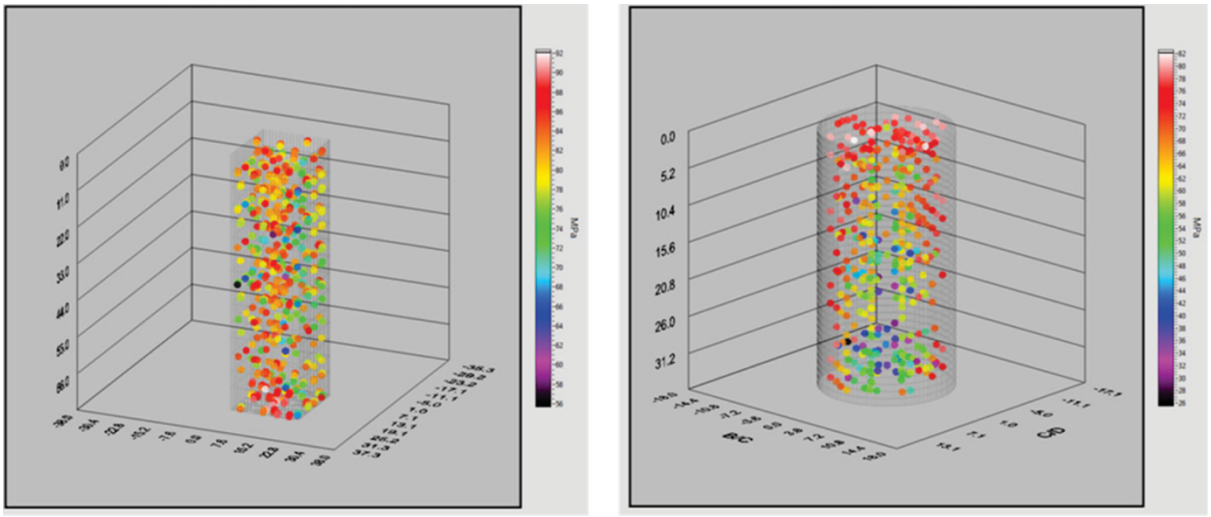

The 3D representation of the compressive strength values for each of the two grades shows a similar qualitative distribution to that seen in the previously evaluated properties, with the compressive strength exhibiting an end-to-end and centre-outside gradient.

IMAGE R

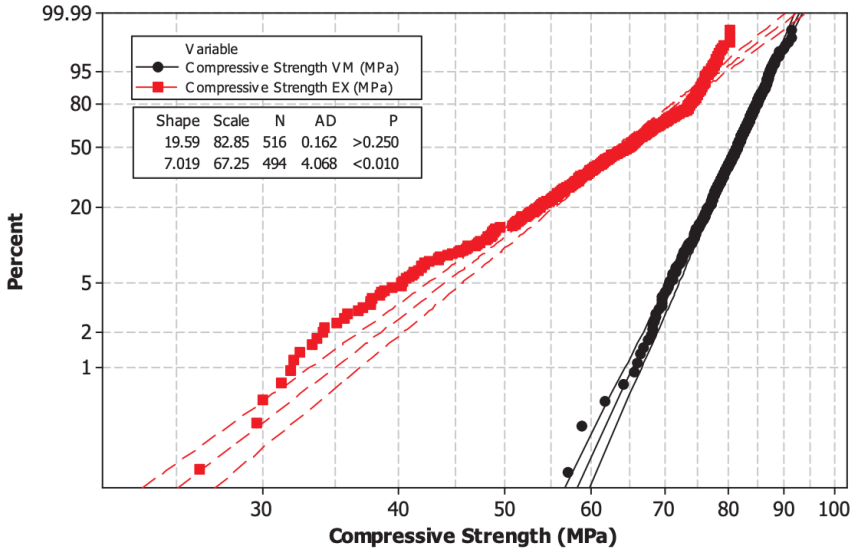

Compressive strength values for the samples tested show greater variability and a lower overall strength distribution in the Imerys grade. The same-grade sample-to-sample variation is shown in Image S. The shape factor actually shows a larger disparity in specific values between the two samples of RSM graphite than is seen for the three samples of Imerys graphite. Despite this, the variability is considerably less overall and within the individual samples for the RSM grade as evidenced by the considerably smaller spread in the distributions, ranging from just under 60 MPa to just over 90 MPa in the RSM graphite and from approximately 30 MPa to 80 MPa for the Imerys grade. A larger spread in compressive strength values is also evident at the lower end of the strength range for the Imerys grade than for the RSM grade; the RSM graphite remains reasonably linear throughout the range of values even when the low outlier strength levels are included.

IMAGE S

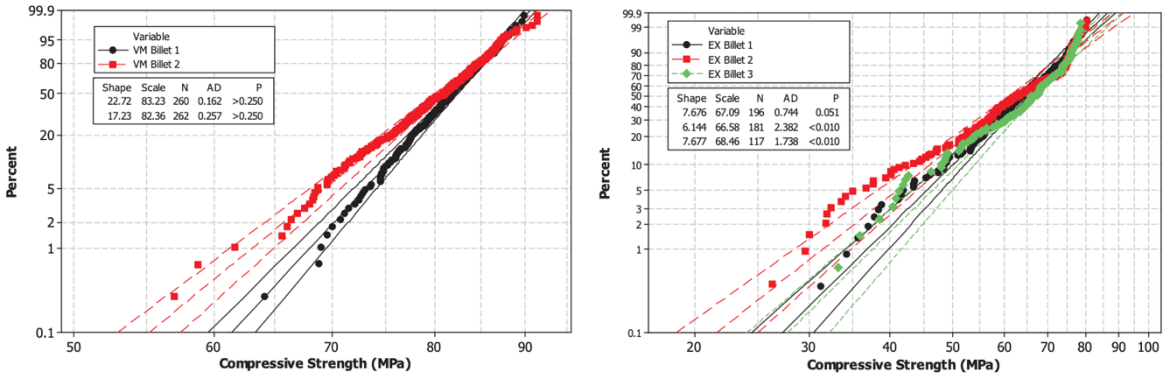

Compressive strength distributions for the RSM samples (left) and Imerys (right) indicate a narrower range of variability for individual RSM graphite than for Imerys.

The orientation effects reveal a slightly different response in the RSM grade when tested in compression compared to the results in tension or flexure. As is shown in Image T (left), the against-grain orientation shows the lowest mean strength level despite being very close in value to the other orientations. The lower range of the distribution also exhibits more scatter than was seen in the tensile and flexural test results, seen qualitatively in the sharp decrease in slope for the against-grain orientation for the data values below the 10th percentile of the distribution. By contrast, the Imerys grade exhibits behaviour very similar to that seen in the other mechanical test results, with relatively non-linear Weibull distributions and considerably less strength in the parallel orientation than is seen in the other two orientations. As with the tensile and flexural strength tests for the Imerys grade, the radial orientation exhibits the highest overall strength distribution.

The main within-sample variability by *z*-axis or sample position for the Imerys grade identified in the density distributions and confirmed in the other mechanical test results is shown in Image U. As can be seen from the boxplot, the trend in variability follows the same pattern from end to end as seen in the other results. The lowest mean values are at the end of the sample opposite the highest mean values with a gradual transition through the entire *z*-axis range.

IMAGE T

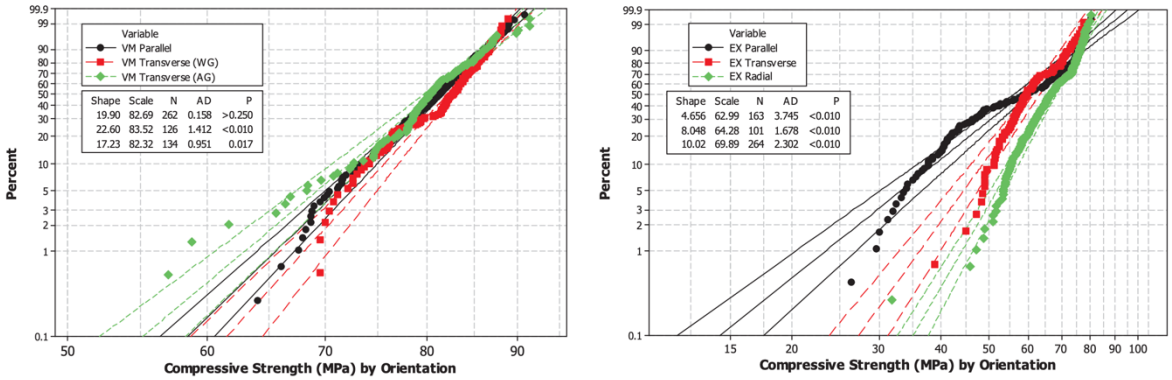

The compressive strength distributions by orientation overlap are consistent at the upper values for the RSM graphite (left), with higher variability and lower overall values for the against-grain orientation in the lower range. The Imerys grade (right) shows the same pattern for mechanical strength as seen previously – the radial orientation is the most consistent and strongest orientation, while the parallel orientation has the weakest distribution of values.

IMAGE U

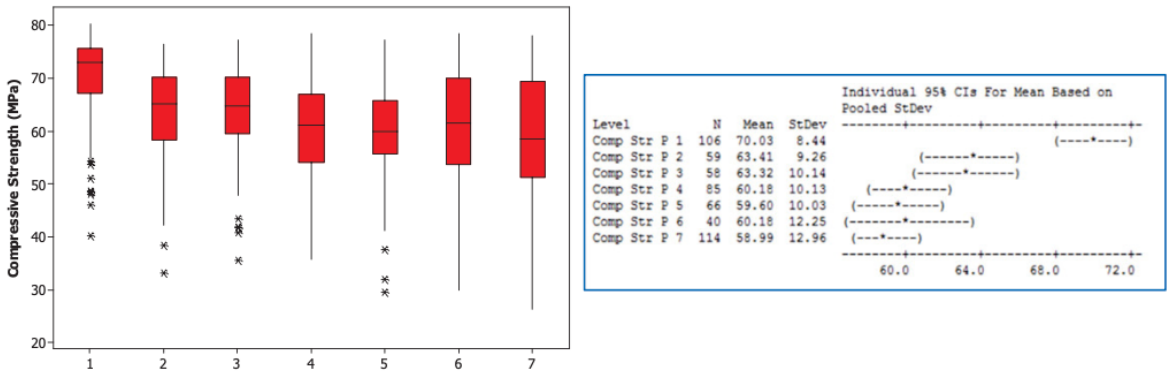

The end-to-end trend variation in the Imerys grade shows the same trend in decreasing values by sample number (left) with confirmation of the variability in mean values shown by an ANOVA evaluation (right).

Discussion

A full breakdown of the property variation is each grade can clearly be broken down into subgroups that yield differences with far greater resolution than is presented by the relatively simple *z*-axis groups evaluated in the previous sections. The density and property variation in the Imerys graphite, for instance, shows gradients in the transverse directions from the centreline as well as the *z*-axis gradient from end to end that was plotted in the previous sections for each of the measured properties. As was seen earlier in this report, the radial orientations had a higher overall strength distribution, so this qualitative observation may be based largely on the artifact that the stronger radial orientation specimens can be extracted closer to the outer edge of the sample. The distribution could therefore be effectively skewed toward larger strength values at the outside positions even though the relative strength of each orientation with respect to distance from the sample centreline might actually remain consistent.

Using the compression testing results as an example and the radial orientations as a specific response group, this variation and presence of a property artifact is readily evaluated by plotting the mean values for compressive strength for the radial specimens by position rows, which are numbered 1 through 5 as the distance from the sample centreline increases along the *x*-*y* plane to the outer sample edge. The boxplot in Image V confirms the higher values at the outermost positions (Row 5) throughout the range of *z*-axis groups even with the orientation effect isolated, confirming that the property gradient along the transverse sample axis exists and is not an artifact of the physical limitations of removing specific geometries at fixed orientations close to the outer edge of the sample. Further breakdowns within these subgroups can be made based upon a qualitative evaluation of the 3D property plot for compressive strength. The grouping within the sample (Image W) that shows the highest distribution of strength values appears to be represented by the entire population of Slab 1 (sample top), while the lowest values for compressive strength are grouped in the “bottom” slabs near the centreline.

IMAGE V

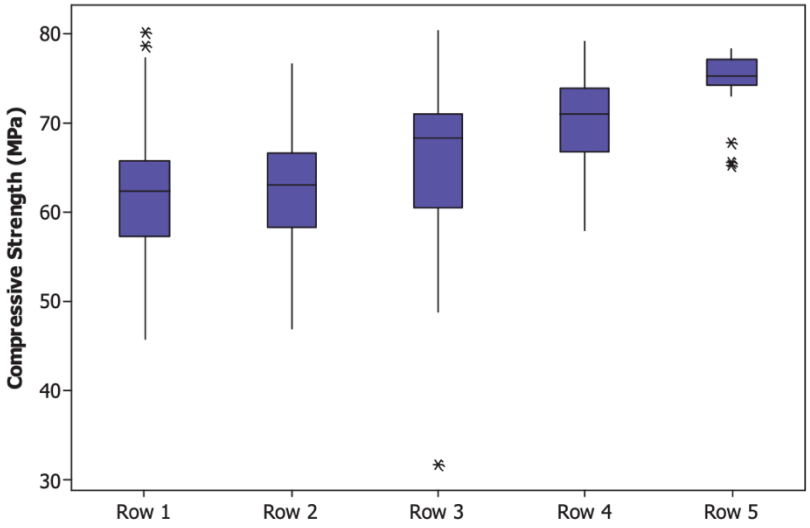

Boxplots confirm the increasing trend in strength values in the radial orientation from centreline to the outer edge of the RSM grade seen qualitatively.

IMAGE W

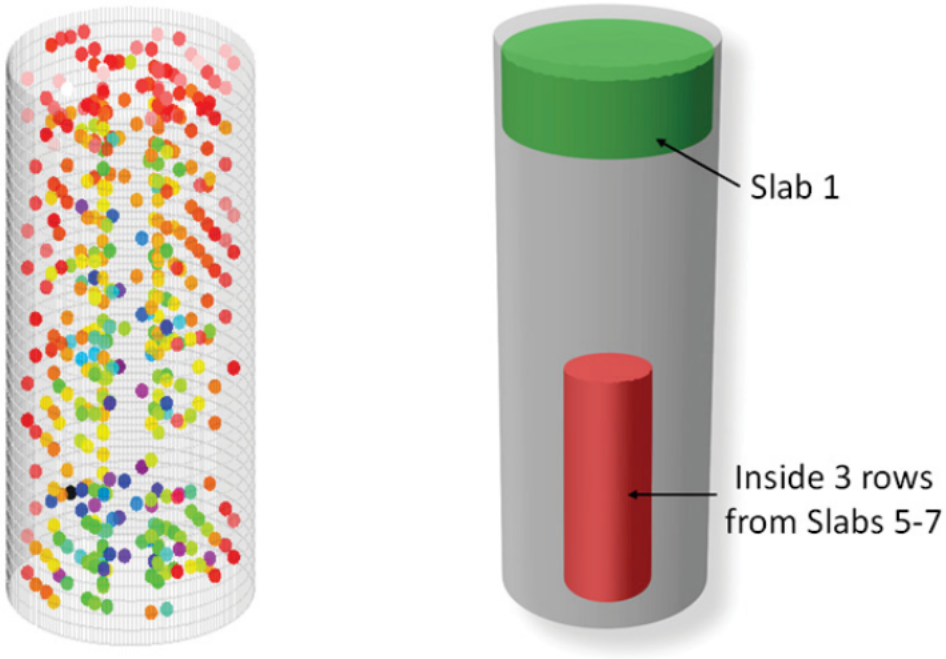

The 3D plot (left) high strength distribution in the upper layer of the RSM sample and a lower strength region in the bottom centre section of the sample. These regions can be quantified by extracting data from the subgroups that compose those specific positions in each of the samples (right).

These two distinct groupings, represented by the green and red sub-sections in Image W (right), demonstrate the global variability in properties within samples of the RSM grade from a more practical application and component-level understanding than would direct comparisons of high and low scalar values with error percentages. Image Y shows a boxplot (a) of the two “extremes” of the grade distribution along with a probability distribution (b) comparing the two groups. Further confirmation of the property relationship to the density distribution is enabled by the large disparity between the two sets of data from within individual samples. The observation that density is a key predictor of properties is not surprising; the variation in measured values is a reflection of the pore, void, and crack population inherent to graphite volumes. The size, shape, and orientation of the larger disparate flaws will also have a distinct effect on measured mechanical properties, even when those flaws result in no actual test data being collected. The within-sample variability of the largest disparate flaw population can be represented through careful tracking of specimens that do not reach the property evaluation phase at all, as finished test specimens from prescribed positions are not possible due to flaws that compromise the specimen coupons prior to completion of the machining process. Large flaws that are on a scale that traverses a considerable fraction (or, in some cases, the entirety) of a coupon or partially machined specimen will result in sample breakage under handling stress. Because these specific positions are tracked using the same codes that track test specimens, a representation of the large disparate flaws can be plotted in the same manner as other properties of interest. Image Z shows the individual positions that were not machined into test specimens due to failure during the handling, extraction and machining process. As can be seen from the representation, the largest disparate flaws are grouped in the same region as the finished specimens with the lowest density and lowest strength values. It is not necessarily the large individual flaws themselves that compromised whole specimens and weakened neighbouring specimens so much as it is an indication of a wider distribution of flaw sizes in those regions that are large enough to compromise measured strength or physical property values.

IMAGE Y

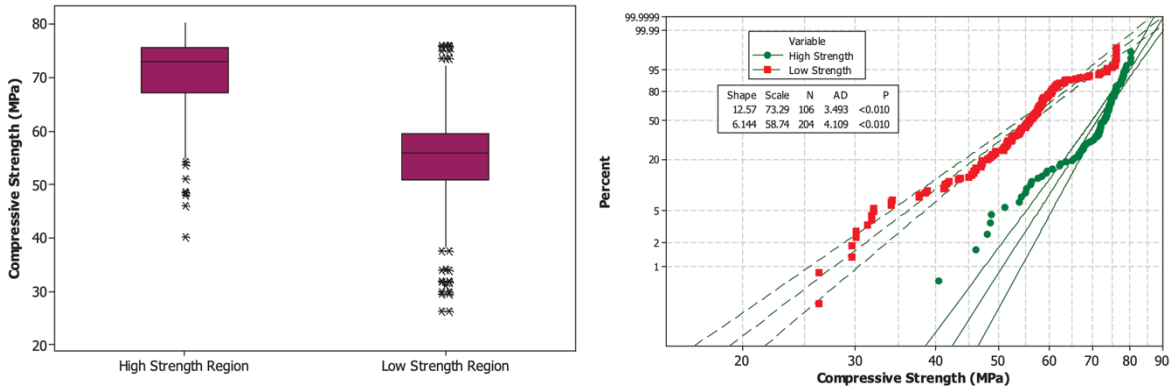

A boxplot of the two regions (left) shows the difference by directed subgroup of the variation from high strength to low strength regions in the RSM graphite. The specific distribution of strength values from each of those regions (right) provides confirmation of the variation and characteristic value levels.

IMAGE Z

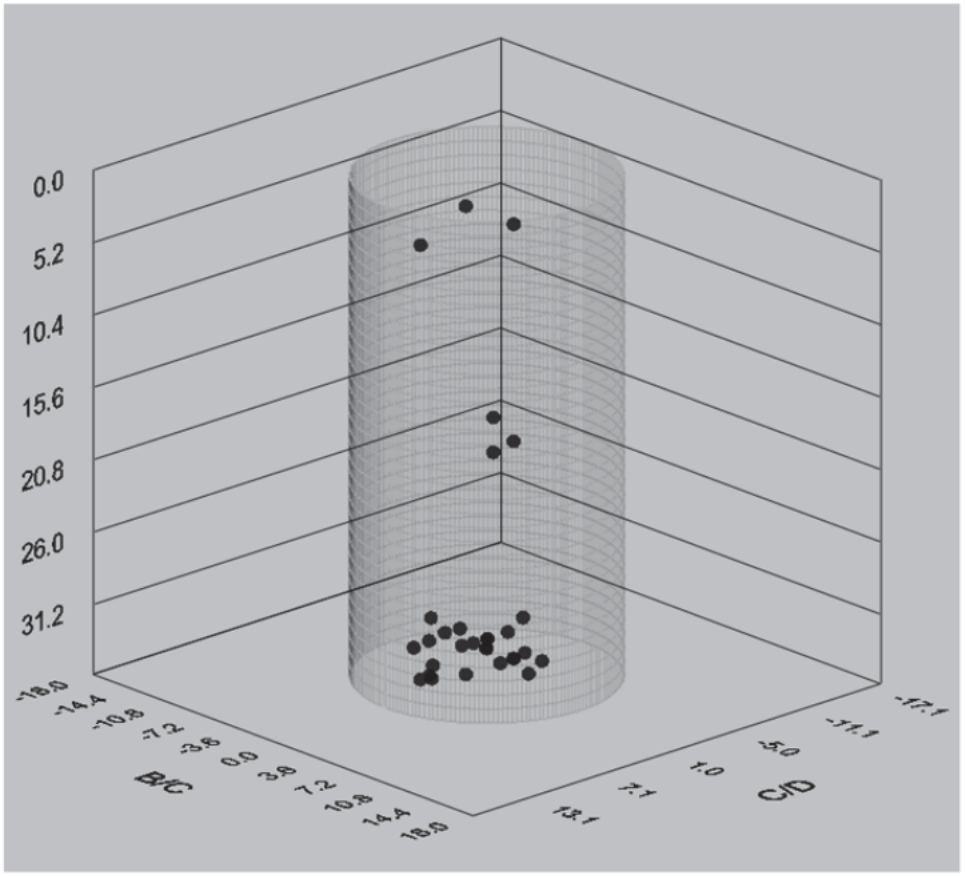

Distribution of the largest disparate flaws based upon the resolution of individual extraction and handling of specimen coupons.

The potential for the continued development of flaw distribution and property relationships becomes more distinct as data continues to be collected and evaluated utilizing similar subgrouping techniques based upon qualitative observations. An understanding of the dependency of strength and performance mechanisms on grade-specific characteristics (raw materials and process techniques) is critical to the optimization of graphite in EV electrode systems, and this understanding begins with the identification of property value variations that are demonstrated to be statistically significant.

SUMMARY

The comparative strength and elastic properties of graphite samples from RSM and Imerys have been compiled based upon the data collected thus far by baseline graphite characterization program. From the 84 mechanical test specimens that have been tested in various forms to date, a number of graphite response characteristics have been quantified that help to elucidate the overall graphite behaviour in the as- manufactured and raw state.

Baseline graphite characterisation is a fundamental viewing window into the projected quality of a graphite sample. Samples with high mean strength and modulus values, consistent distribution of property gradients and low flaw size, will typically also demonstrate characteristics that are regarded as key properties of high-quality electrode materials. These include, but are not limited to, porosity, coefficient of thermal expansion, thermal conductivity, specific heat capacity and electrical resistivity.

The mean strength and modulus values are higher in the RSM graphite than the Imerys grade in all of the properties evaluated in this report except flexural strength and are considerably more predictable based upon the relative data scatter between the two grades. The distribution of property values based upon position within the original RSM sample is also much more consistent throughout, compared to the Imerys sample. A qualitative analysis of properties through 3D representations is confirmed through quantitative analyses based upon Weibull probability distributions and comparisons of mean values based upon grade-and sample-specific subsets of property values. The basic manufacturing variables in electrode-grade graphite, filler type, particle size, and compaction process, are compared side by side and indicate distinct regions of property gradients within the Imerys graphite that are not as clear from the relatively homogenous property distributions within the RSM grade. Homogenous distribution is a very desirable characteristic in the production of electrodes. This is hugely encouraging when we consider that the RSM sample, which is predominantly homogenous in its composition, is effectively a raw material, that hasn't even been adapted or enhanced for sale purposes. The likely effect of non-homogenous variables would be increased flaw size and erratic density, leading to potentially hazardous hot spots in situ. The distribution in the final sample is apparent from a comprehensive evaluation of property values.

The resolution of distinct subsets of data, as have been analyzed in this report, will continue to evolve as the number of data points representing physical or mechanical property values continues to increase. Data is still being collected on these grades as well as other candidate grades of graphite that differ in raw material, particle size, and manufacturing process. Further evaluation in this pproject will rely on larger and larger datasets that allow conclusions to be drawn concerning the design basis for utilization of RSM grades in battery applications.

This baseline study is hugely encouraging and strongly indicates that more granular studies that will start in January 2022, will liberate comprehensive data that will show explicitly that the graphite samples from RSM are an extremely desirable material in terms of electrode manufacturing. A collaboration as part of a composite material has very interesting and exciting potential.

Paul Adams

December 2021